Cellular Physiology and Biochemistry

Cell Physiol Biochem 2020;54:493-507
DOI: 10.33594/000000232
Published online: 16 May 2020
Accepted: 30 April 2020

Original Paper

Status Epilepticus Dynamics Predicts Latency to Spontaneous Seizures in the Kainic Acid Model

Anna Maria Costa Chiara Lucchi Cecilia Simonini Ítalo Rosal Lustosa Giuseppe Biagini

Department of Biomedical, Metabolic and Neural Sciences, University of Modena and Reggio Emilia, Modena, Italy

Key Words
Epileptogenesis • Gamma power • Kainic acid • Status epilepticus • Temporal lobe epilepsy • Theta power

Abstract
Background/Aims: Status epilepticus (SE) might be followed by temporal lobe epilepsy (TLE), a common neurologic disorder characterized by spontaneous recurrent seizures (SRSs). However, the relationship between SE and TLE is still incompletely characterized. For this reason, in a model of TLE we evaluated the lesion extent and the onset of SRSs to determine if they were influenced by the SE dynamics. ***Methods:*** Sixty-two adult male Sprague-Dawley rats were implanted for video-electrocorticographic (v-ECoG) monitoring and intraperitoneally treated with saline or kainic acid (KA, 15 mg/kg) at 8 weeks of age. v-ECoG recordings were obtained during SE, in the following 9 weeks, and assessed by amplitude or power band spectrum. Rats were euthanized 3 or 64 days after SE to evaluate the lesion. ***Results:*** SE lasted about 10 h during which the mean duration of convulsive seizures (CSs) increased from 39 s, at 30 min, to 603 s at 4 h. The gamma power peaked 30 min after the SE onset and its peak was correlated (r^2=0.13, p=0.042) with the overall SE duration. Subsequently, the gamma power was reduced under the baseline until the end of SE. The theta power increased at approximately 150% of basal levels 3 h after KA injection, but it went back to basal levels with the full development of CSs. Interestingly, the timing of the first SRS in chronic epilepsy was correlated with the latency to develop the first CS with loss of posture during SE (r^2=0.60, p<0.001). Additionally, the overall duration of CSs observed during SE was related to the number of damaged brain regions (r^2=0.60, p=0.005), but it did not influence the timing of the first SRS in chronic epilepsy. ***Conclusion:*** Overall, our results show that the onset of chronic epilepsy is modulated by SE dynamics, whereas brain damage is related to prolonged convulsions in SE.

Giuseppe Biagini, MD
Dipartimento di Scienze Biomediche, Metaboliche e Neuroscienze, Università di Modena e Reggio Emilia Via Campi 287, 41125 Modena (Italy)
Tel. +39 059 205-5747, Fax +39 059 205-5363, E-Mail gbiagini@unimore.it

Introduction

Temporal lobe epilepsy (TLE) is a major neurologic disorder characterized by spontaneous recurrent seizures (SRSs) which often follow a presumably causative lesion, also known as the "initial precipitating injury" [1]. The SRSs begin after a period named "epileptogenesis" during which degeneration and repair, inflammation and aberrant structural phenomena occur in consequence of the initial precipitating injury [2]. It is currently undetermined which one of the various, possible mechanisms able to contribute to epileptogenesis could be critical for the appearance of SRSs in TLE, and all of them have been addressed in a variety of *in vivo* models reproducing seizures or epilepsy, following a wide-spectrum approach [3].

Among other hypotheses, it has been proposed that epileptogenesis could be related to the extension of lesions caused by the initial precipitating injury, especially in the hippocampus [4–6]. This hypothesis was tested in status epilepticus (SE) models by controlling the initial precipitating injury with drugs able to limit the duration of SE to progressively shorter time intervals, so as to obtain a different lesion extent. The prediction made in these experiments was of a possible change in the latency to first SRS in response to the reduction in SE duration. However, the results paradoxically showed both delay and anticipation of SRSs in presence of reduced hippocampal damage [4, 6]. Conversely, in a different study authors did not find differences in the period of time required to the onset of SRSs in rats exposed to a short (30 min) or prolonged (120 min) period of SE [7]. In all of these experiments pilocarpine was the proconvulsant used to trigger the SE [4, 6, 7].

Using kainic acid (KA) to model SE [8–12], authors differently approached the relationship between SE and epileptogenesis. Specifically, the onset of convulsive seizures (CSs) in the course of SE (hereafter defined as convulsive SE, CSE) [13] was considered as the possible determinant of SRS onset, independently of the lesion extent [8]. Anyway, also in this case no correlation between the latency to CSE and time required to develop the SRSs was found in animals surviving to KA. A possible explanation to these approaches failing in the tentative to establish a relationship between SE and epileptogenesis could be that all the animals were treated with drugs able to limit the SE duration and inducing neuroprotection. In such a way, drug treatment could have modified the course of subsequent epileptogenesis by interfering with the initial precipitating injury.

To get further insights into the relationship between SE, damage and epileptogenesis in the KA model, we designed experiments without any drug administration to fully characterize the dynamics of SE and the onset of SRSs by video-electrocorticographic (v-ECoG) recordings. Additionally, we also localized the lesions and measured their extension to establish a relationship with the SE dynamics. Finally, we investigated the relationship between epileptogenesis and lesion extent or SE dynamics. Here, we show that some characteristics of SE could be useful in predicting the brain damage and timing of epileptogenesis.

Materials and Methods

Animals

A total of 62 male Sprague-Dawley rats (Charles River, Calco, Italy) with initial weight of 175-200 g were used in this study. Animals were housed in a specific pathogen-free facility with controlled environment conditions and ad libitum access to water and food. All experiments were authorized (323/2015-PR) and performed according to the European Directive 2010/63/EU. The local Animal Welfare Body approved the study protocol. All efforts were done to refine procedures, improve the welfare and reduce the number of animals.

Experimental design

Animals were randomly divided into two groups to investigate the lesions (n=34) or epileptogenesis (n=28). The first group consisted of 17 rats that received an injection of KA (15 mg/kg, i.p.; Sigma-Aldrich,

Milan, Italy) compared with 17 controls receiving an i.p. injection of saline (1 ml/kg). These rats were euthanized after 3 days from the injection at 8 weeks of age (11 KA-treated rats and 11 controls) to evaluate early brain injuries, or 64 days after injections at 17 weeks of age (6 KA-treated rats and 6 controls) to evaluate the presence of chronic brain injuries. The second group included KA-treated rats used to evaluate the relation between SE and epileptogenesis, and monitored until 17 weeks of age. All rats were treated with KA or saline one week after electrode implantation. At the end of SE, rats were given a subcutaneous (s.c.) injection of Ringer's lactate solution (3–5 ml) and softened rat chow to minimize animal discomfort.

v-ECoG recordings

As described previously [14], rats were implanted with epidural electrodes in frontal and occipital cortices, in order to continuously record ECoG data of both hemispheres. One electrode was implanted below the lambda on the midline in all animals and used as a reference. For electrode implantation, deep anesthesia was induced with volatile isoflurane and assessed by deep breath, loss of tail and eye reflexes. At the end of the surgery, gel containing 2.5 g lidocaine chloride, 0.5 g neomycin sulfate and 0.025 g fluocinolone acetonide (Neuflan® gel; Molteni Farmaceutici, Scandicci, FI, Italy) was applied to reduce acute pain and risk of infection. All animals were monitored until complete recovery from anesthesia and housed in single cages with no grids or environmental enrichments to reduce risk of headset loss. Following guidelines [15], the EcoG was recorded via cable connection between headset and preamplifiers. Electrical brain activity was digitally filtered (0.3 Hz high-pass, 500 Hz low-pass), acquired at 1 kHz per channel, and stored on a personal computer after the mathematical subtraction of traces of recording electrodes from trace of reference electrode, using a PowerLab8/30 amplifier connected to 4 BioAmp preamplifiers (ADInstruments; Dunedin, Otago, New Zealand). Videos were digitally captured through a camera connected to the computer and synchronized to the ECoG traces through LabChart 8 PRO internal trigger. Baseline ECoG was recorded at least 24-48 h prior to the treatment. Both control and KA-treated rats were recorded in the same manner and data analyses were performed with blind procedures.

Behavioral and ECoG analysis

ECoG traces were digitally filtered offline (band-pass: high 50 Hz, low 1 Hz) and manually analyzed using LabChart 8 PRO software (AD Instruments) by blind to treatment expert raters. Based on the definitions provided in the literature [8, 16, 17], all seizures were defined as ECoG segments with minimum duration of 10 s, continuous synchronous high-frequency activity, and amplitude at least twice as the previous baseline. These ECoG segments were also screened for the appearance of a post-ictal depression (below baseline ECoG activity). Seizures and their durations were determined in the ECoG traces, and then investigated for a behavioral correlate [18] by using the synchronized video recordings. Particularly, seizures were scored as stage 0 (or subclinical) if a clear epileptiform ECoG signal was present without corresponding evident behavior in the video; stage 1-2 in presence of absence-like immobility, "wet-dog shakes", facial automatisms, and head nodding; stage 3, when presenting with forelimb clonus and lordosis; stage 4, corresponding to generalized seizures with rearing; and stage 5, when seizures consisted of rearing with loss of posture and/or wild running, followed by generalized convulsions. SE was defined as the period of time in which rats either did not recover normal behavior between one seizure and the other, or in which they displayed continuous shaking for more than 5 min [19]. The end of SE was characterized by a progressive reduction in frequency of the continuous electrographic spikes, preceding a silent period. Moreover, the termination of SE was accompanied by recovery of normal behavior. According to the definition of "early seizure" provided in literature [12], we considered the ictal events as "early", i.e. additional KA-induced seizures when occurring in the next few days after KA administration. In agreement with Williams and colleagues [20], initiation of the first SRS was defined by a single, large ECoG spike, followed by large high-frequency activity. The progression was characterized by individual spike-like events followed by regular, large, high-frequency events. At the end of this activity, large-amplitude waves with multiple superimposed spike-like events were followed by a silent period. Artifacts were carefully removed from the v-ECoG analysis of SRSs. They were identified as (i) high frequency signals associated with masticatory movements in the video recording, (ii) interference appearing as a thickening caused by superposition of 50 Hz mains in the ECoG; (iii) electrode or cable-related technical artifacts. The amplitude spectrum maps, in which amplitude gives a spectrum where the height at a particular frequency is the amplitude at that frequency, were respectively reported as the first nonconvulsive and the first convulsive SRS. Then, ECoG traces were further analyzed

using EDFbrowser (1st order butterworth high-pass filter: 1Hz; powerline interference removal: 50 Hz) [21] to understand whether significant changes in the cortical power band spectrum occurred during the SE. A relative indication of the distribution of power over the frequency regions ranging from 1 to 100 Hz, expressed in percentage (%) and recorded from the frontal electrodes, were determined. Frontal electrodes were preferred because gamma oscillations were shown to be present in the frontal and parietal areas [22], while theta oscillations were particularly pronounced in the frontal midline [23–27] and in the subcortical areas [28–31]. Thus, the power band spectrum analysis was expressed in percentage and included delta (δ, 0–4 Hz), theta (θ, 4–8 Hz), alpha (α, 8–12 Hz), beta (β, 12–24 Hz), and gamma (γ, 24–100 Hz) frequencies in 10-s epochs on a continuous ECoG during 12 h after KA treatment.

Immunohistochemistry

Control rats and rats treated with KA were used for tissue analysis. Rats deeply anesthetized with isoflurane were transcardially perfused with phosphate buffered saline (PBS, pH 7.4) followed by Zamboni's fixative (pH 6.9), 3 or 64 days after treatment. Brains were post-fixed at 4°C in the same fixative for 24 h, cryoprotected in 15% and 30% sucrose solutions [32] and stored at −80°C until use. Horizontal sections of 50 µm were cut using a freezing sliding microtome (Leica SM2000R; Leica, Nussloch, Germany). As described previously [32, 33], sections were washed three times in PBS, treated with 3% H_2O_2 in PBS (20 min), and blocked 1 h with 5% normal goat serum (NGS) in PBS containing 0.1% Triton X-100 (PBS-T). Sections were incubated overnight at 4°C in PBS-T containing 1% NGS, respectively with the following antibodies: mouse anti-neuron-specific nuclear protein (NeuN, Millipore, #MAB377 clone A60, 1:200) and mouse anti-glial fibrillary acidic protein (GFAP, Sigma Aldrich, #G3893, 1:500). The next day, sections were incubated 1 h with secondary antibody (biotinylated horse anti-mouse; Vectastain, 1:200). All sections were then processed by the avidin-biotin-peroxidase complex (Elite ABC Kit; Vector Laboratories). Immunostaining was performed in 0.05% 3, 3-diaminobenzidine tetrahydrochloride (DAB, Sigma-Aldrich) for 5 min and developed by adding 0.03% H_2O_2. Finally, the sections were washed in PBS, mounted on gelatin-coated slides and coverslipped with Eukitt® (O. Kindler GmbH & Co).

Fluoro-Jade B

As described previously [32], sections were mounted on gelatin-coated slides and dried at room temperature. Slides were immersed for 5 min into a solution containing 1% sodium hydroxide in 80% ethanol, washed for 2 min in 70% ethanol followed by 2 min in distilled water, before being oxidized in 0.06% potassium permanganate for 15 min. Brain sections were then stained for 15 min in 0.004% solution of Fluoro-Jade B (FJB, Millipore, # AG310-30MG) diluted in 0.1% acetic acid. Slides were rinsed in deionized water for 3 min, dried on a pre-warmed hotplate at 50°C, then cleared in xylene and coverslipped with Eukitt®. Images were acquired using a Leica SP2 AOBS confocal microscope.

Image analysis

Immunostained sections from −8.04 mm to −5.04 mm Bregma level were evaluated with a Nikon Eclipse CiL (Nikon Instruments) at 10X and for each area of interest (Cornu Ammonis 3 stratum pyramidalis - CA3 Py, subregion B; hilus of the dentate gyrus – DH; subiculum – Sub; layer III of the medial entorhinal cortex - MEnt L.III; nucleus reuniens – Re; anterior olfactory nucleus - AOP) images were digitally captured by a Nikon DS-Fi3 digital camera. The number of NeuN immunoreactive cells and the FJB-positive cells per mm^2 were quantified and analyzed using the ImageJ software. Particularly, FJB-positive cells were evaluated only in regions in which we localized pannecrosis, as identified by loss of astrocyte GFAP immunostaining. The area selected for each region of interest (ROI) was consistent in all analyzed sections. The image analysis software NIS-Elements was used to manually trace the unstained area upon GFAP detection in the CA3 lacunosum-molecolare (CA3 LMol), as well as in Sub, Re and AOP. To estimate the extent of hippocampal atrophy in epileptic rats, we used the same software, by measuring the ratio between the hippocampal area (from CA3 to CA1, DG, Sub and, excluding the fimbria) and the total brain area (excluding the cerebellum).

Statistics

v-ECoG analysis and the relative distribution of power over the frequency expressed in percentage were both investigated using a one-way repeated measures analysis of variance (ANOVA). Multiple comparisons versus the control group (Dunnett's test) were performed to establish differences between time intervals

considered after the induction of SE and a reference starting point, respectively set at 0.5 h in the v-ECoG analysis and 0 h in the power band spectrum analysis expressed in percentage. For immunohistochemical analysis, the statistical comparison between groups was performed using the Student's t-test or one-way ANOVA followed by the Holm-Sidak test. Linear regression was used to model the relationship between two normally distributed variables. Statistical analyses were performed with SigmaPlot 13 (Systat Software). Data are represented as means with standard error of the mean (SEM).

Results

General outcomes of the KA model

Stage 0-2 nonconvulsive seizures (NCSs) were observed after approximately 14 min from KA administration. The first stage 3 seizure appeared after another additional 23 min, whereas the first CS (stage 4 or 5) required a time interval of approximately 1 h. When considering stage 5 seizures only, the first occurred at 80 min from treatment. According to our definition, SE was attained at approximately 45 min from KA injection and lasted on average for 10 h. Importantly, almost all rats (93%) developed the SE, and mortality was 4%. After the SE, "early seizures" were generally NCSs observed with 24 h after SE termination in 20% of rats. After 10 days, 97% of rats developed SRSs. The first stage 4 or 5 convulsion was observed 18 days after KA treatment. When considering stage 5 only, the first seizure appeared after 3 weeks at average (Table 1).

Characterization of the duration and progression of CSs during SE

Significant differences in the duration of stage 4 seizures were found by comparing the 0.5 h time interval with, respectively, 2 h, 2.5 h, and 3 h intervals ($p<0.05$ for all of them, Dunnett's test). Accordingly, significant differences were also found for the duration of stage 5 seizures, which were longer in the 3.5 h and 4 h time intervals than in the 0.5 h interval ($p<0.05$). By summing up the duration of stage 4 and 5 seizures, significantly higher values were found for 2.5 h, 3 h, 3.5 h, and 4 h compared to the 0.5 h time interval ($p<0.05$) (Fig. 1A).

The development and evolution of SE

The percentage of gamma power significantly increased 30 min after the administration of KA (time 0 h vs 0.5 h, $p<0.05$; Dunnett's test), but then declined from 1 h to 3 h and 4 h, and also from 5 h to 11 h ($p<0.05$ for all time intervals vs 0 h) before to return to baseline at later time intervals. Conversely, the percentage of theta power progressively increased from 0.5 h to 3 h, being significant at 2.5 h and 3 h ($p<0.05$) in the case of stage 4 seizures (Fig. 1B). Interestingly, the gamma power measured 30 min after the KA injection significantly correlated with total duration of SE ($r^2=0.13$, $p=0.042$) (Fig. 1C), but not with the latency to develop

Table 1. Timing of seizure onset during status epilepticus (SE) and chronic epilepsy after kainic acid (KA) treatment. ECoG, electrocorticography; SRS, spontaneous recurrent seizure; st., stage

Response to KA injection	Latency, duration and percentage of response
First st. 0-2 ECoG seizure	14.37 ± 2.10 (min)
First st. 3 ECoG seizure	37.27 ± 4.21 (min)
First convulsive st. 4 or st. 5 ECoG seizure	58.55 ± 4.22 (min)
First st. 5 ECoG seizure	81.15 ± 6.34 (min)
SE	47.22 ± 2.15 (min)
SE (duration)	10.12 ± 0.45 (h)
Rats developing SE	93%
Rats died during or after KA injection	4%
Rats developing "early seizures" after KA treatment	20%
Rats developing SRSs	97%
First ECoG SRS	9.96 ± 0.95 (days)
First convulsive st. 4 or st. 5 ECoG SRS	18.18 ± 2.60 (days)
First convulsive st. 5 ECoG SRS	21.25 ± 3.04 (days)

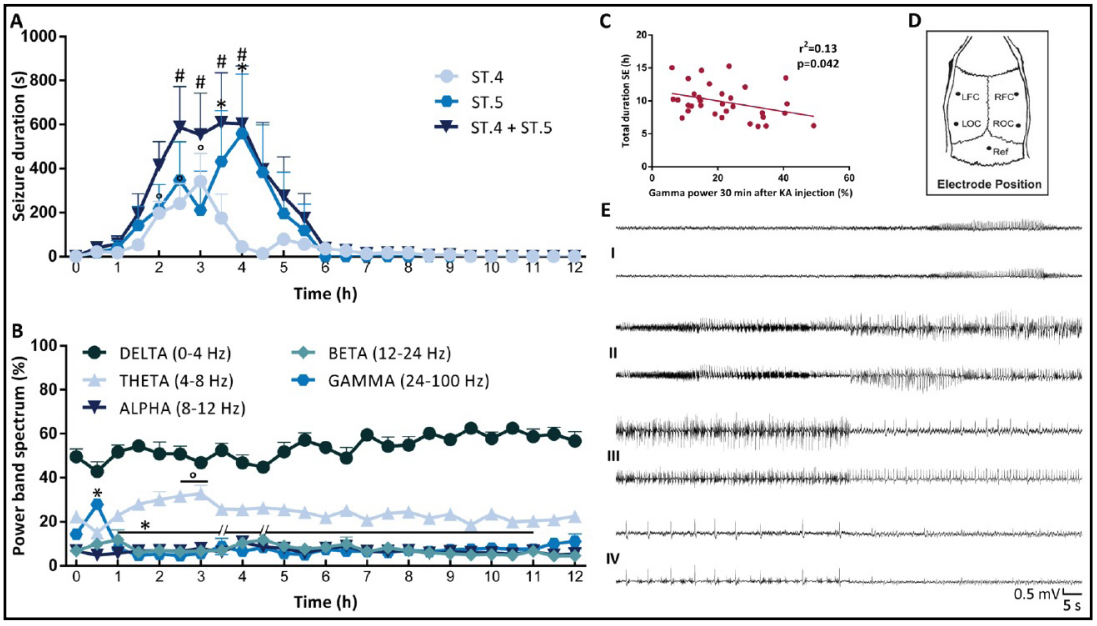

Fig. 1. Behavioral and electrographic changes observed during status epilepticus (SE). In A, significant differences in the duration of stage (st.) 4 and 5 convulsive seizures were determined during 12 h after the administration of kainic acid (KA). In B, a relative indication of distribution of power over the frequency, expressed in percentage, was determined during 12 h after the administration of the KA. In C, a linear regression (r^2) between the gamma power at 30 min after the administration of KA, and the total duration of SE is illustrated. In D, the position of frontal and occipital electrodes is shown. In E, the development and evolution of SE in the KA model were reported. Particularly, the baseline and then the first nonconvulsive seizure is represented in E.I. The progression from nonconvulsive SE to convulsive SE is reported in E.II. The evolution of SE over time is represented in E.III. The interictal spikes appearing at the end of SE and then the return to baseline are reported in E.IV. Statistical analysis was performed using a one-way repeated measures analysis of variance (ANOVA) followed by multiple comparisons versus control group (Dunnett's test). Data are shown as mean ± SEM. ° $p<0.05$ (st. 4), * $p<0.05$ (st. 5), # $p<0.05$ (st. 4 + 5); Scale: 0.5 mV/5 s. LFC, left frontal cortex; LOC, left occipital cortex; Ref, reference electrode; RFC, right frontal cortex; ROC, right occipital cortex.

SRSs ($r^2=0.07$, $p=0.199$) (data not shown). Electrographic traces, recorded from frontal and occipital traces (Fig. 1D), were reported in Fig. 1E (I-IV) to illustrate the SE.

Neuronal cell damage after SE induction

In contrast to control rats of 8 weeks of age, damaged neurons positive to FJB were found throughout the brain of 8-week-old rats treated with KA (Fig. 2A and B). Particularly, highest densities of FJB-positive cells were found in AOP and MEnt (L.III); intermediate cell damage was in Re, CA3 Py (subregion B), and Sub; lower values characterized the DH (Fig. 2C and D).

Neuronal cell survival after induction of SE and development of SRSs

Concerning cell survival (Fig. 3A), neurons were significantly reduced to 56% ($p<0.001$, 3 days post-SE vs age-matched controls; Holm-Sidak test) and, respectively, 72% ($p<0.001$, epileptic animals vs age-matched controls) of control CA3 Py (subregion B) levels (Fig. 3B). In the DH, neurons were reduced to 63% of control rats in rats treated with KA and studied 3 days after the SE ($p=0.002$). Similarly, in the same brain region, neurons were reduced to 49% of corresponding controls 64 days post-SE ($p<0.001$) (Fig. 3C). The Sub was also significantly damaged, as neurons were 62% ($p<0.001$) of control levels at the earlier time interval, whereas they decreased to 75% of controls at 64 days post-SE ($p=0.011$) (Fig. 3D).

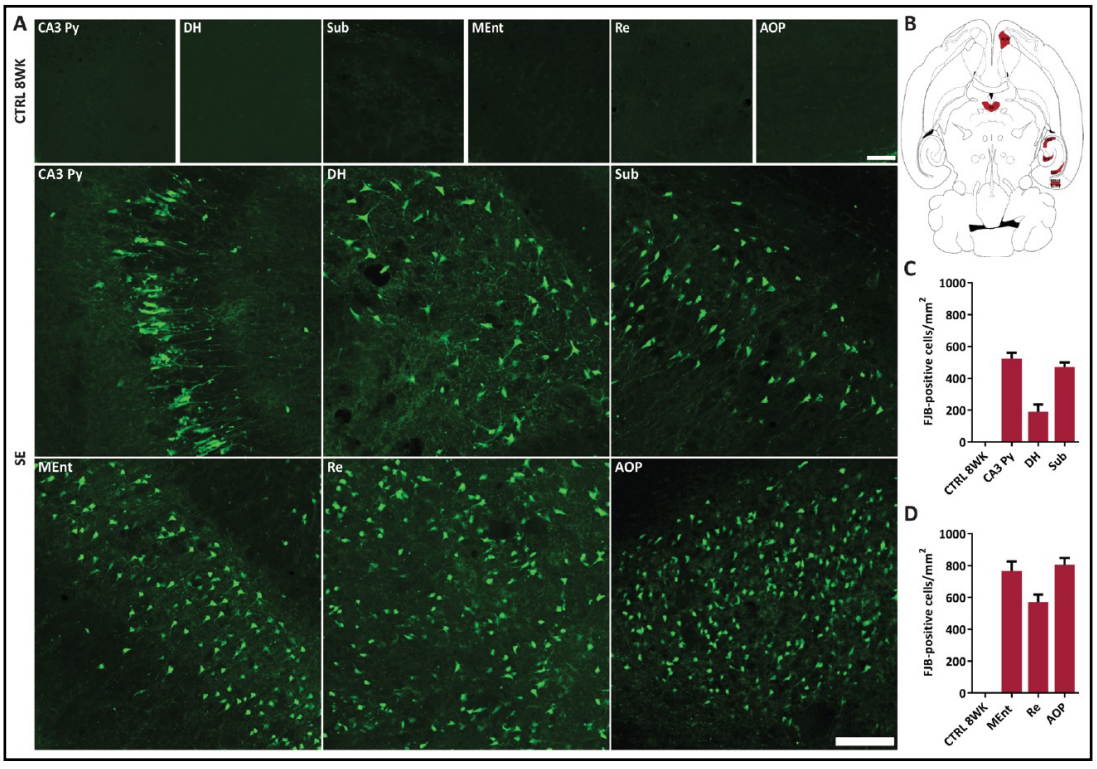

Fig. 2. Neuronal cell death after induction of status epilepticus (SE) in kainic acid (KA) model. Sections were stained for Fluoro-Jade B (FJB) to evaluate neuronal cell death (A) in several brain regions (B). The KA treatment induced a significant increase, compared to control group (CTRL) of 8 weeks of age, in FJB staining in the CA3 stratum pyramidalis (CA3 Py, subregion B), hilus of the dentate gyrus (DH) and subiculum (Sub) (C), as well as in layer III of the medial entorhinal cortex (MEnt L.III), nucleus reuniens (Re) and anterior olfactory nucleus (AOP) (D). Quantification was performed using ImageJ. Data are shown as mean ± SEM. Scale bar: 100 μm. WK, week.

In the MEnt (L.III), neuronal counts were acutely lowered to 56% of control levels ($p<0.001$), and to 52% of age-matched controls in the epileptic rats ($p<0.001$) (Fig. 3E). Concerning the Re, neurons decreased to 56% in KA-treated animals vs age-matched controls ($p=0.003$), and to 40% in epileptic rats ($p<0.001$) (Fig. 3F). Finally, a similar decrease in neuronal counts was also observed in the AOP, in which cells were 63% of controls ($p<0.001$) in rats at 3 days after SE, and 50% in epileptic rats ($p=0.004$ vs age-matched controls) (Fig. 3G).

GFAP-immunonegative areas in the brain after induction of SE

Accordingly to the literature [34, 35], when compared to controls (Fig. 4A-B) rats treated with KA presented a mean lesion which respectively was 0.13 ± 0.05 mm^2 in CA3 LMol, 0.10 ± 0.02 mm^2 in Sub, 0.43 ± 0.14 mm^2 in Re and 0.64 ± 0.05 mm^2 in AOP. As shown in Fig. 4C, we also calculated the percentage of the lesion in respect of the total area, evaluated in brain sections stained with NeuN to clearly identify the selected regions. The percentage covered by the lesion respectively was 24% in CA3 LMol, 18% in Sub, 45% in Re and 78% in AOP.

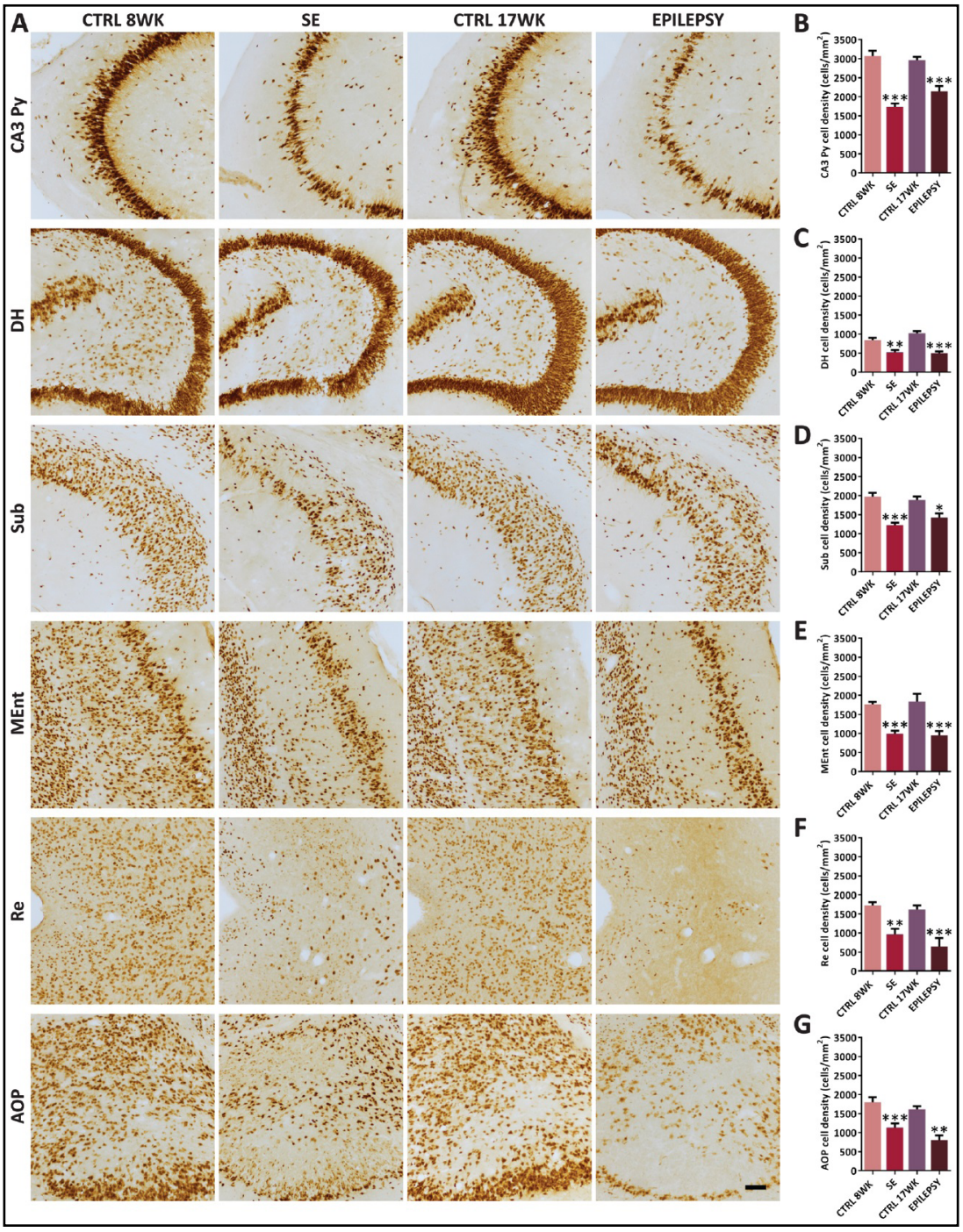

Fig. 3. Neuronal cell survival after induction of status epilepticus (SE) in the kainic acid (KA) model. Brain sections were stained against mouse anti-neuron-specific nuclear protein (NeuN) to evaluate neuronal cell survival (A). The KA treatment induced a significant decrease, compared to control group (CTRL), in the number of NeuN-positive cells in the CA3 stratum pyramidalis (CA3 Py, subregion B) (B), hilus of the dentate gyrus (DH) (C), subiculum (Sub) (D), layer III of the medial entorhinal cortex (MEnt L.III) (E), nucleus reuniens (Re) (F) and anterior olfactory nucleus (AOP) (G). This significant decrease in the number of NeuN-positive cells is present 3 (8 weeks of age) and 64 (17 weeks of age) days after the KA administration. Quantification was performed using ImageJ. Statistical analysis was performed using a one-way ANOVA followed by all pairwise multiple comparison procedures (Holm-Sidak test). Data are shown as mean ± SEM.* $p<0.05$, ** $p<0.01$, *** $p<0.001$; Scale bar: 100 µm. WK, week.

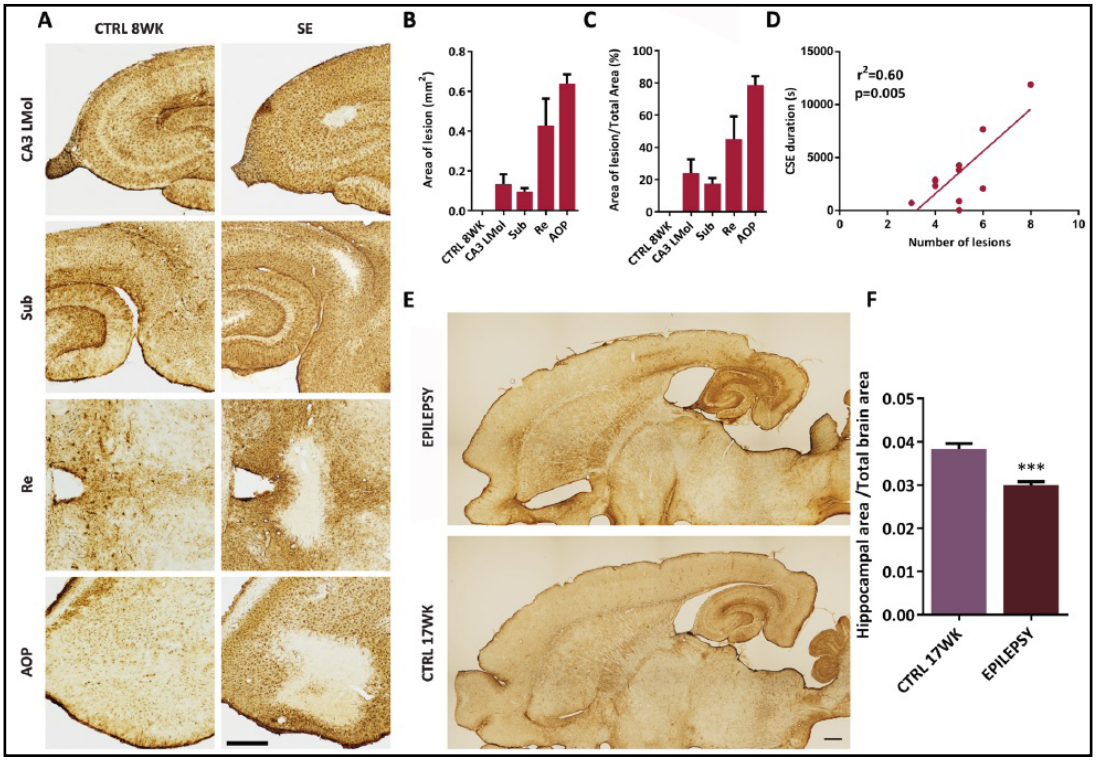

Fig. 4. Lesioned areas and hippocampal atrophy in kainic acid (KA) model. Brain sections were stained against mouse anti-glial fibrillary acidic protein (GFAP), a marker of astrocytes, which are absent in lesioned areas (A). Comparing to control group (CTRL) of 8 weeks (WK), the KA treatment induced GFAP-immunonegative areas in CA3 stratum lacunosum-molecolare (CA3 LMol), subiculum (Sub), nucleus reuniens (Re) and anterior olfactory nucleus (AOP) (B). In C, the percentage of lesion area of the total area was also determined in CA3 LMol, Sub, Re and AOP. In D, the linear regression (r^2) between the number of damaged brain areas and mean duration of convulsive seizures during status epilepticus (SE) was also determined. The hippocampal atrophy of 64-week-old rats (E) was measured in F. Quantification of the area was performed using the image analysis software NIS-Elements. Statistical analysis was performed using a linear regression analysis and a Student's t-test. Data are shown as mean ± SEM. ***p<0.001; Scale bars: 500 µm and 1 mm. CSE, convulsive status epilepticus.

Relationship between the duration of CSE and the number of damaged areas within the brain

Three days after SE induction, the percentage of rats presenting lesions revealed by loss of GFAP immunostaining were, respectively, 100% for Sub and AOP, and 64% for CA3 LMol and Re. Additionally, we found that 73% rats were damaged in CA3 Py (subregion B), 27% in CA1 Py, amygdala and entopeduncular nucleus, 9% in CA1 stratum radiatum and substantia nigra. After having calculated the total number of brain lesions for each animal, we tested the relationship between duration of CSE and number of damaged areas, finding a significant relationship between total duration of CSs (stage 4 and stage 5) and the number of damaged areas (r^2=0.60, p=0.005) (Fig. 4D). At variance, no significant correlation was found between the total duration of SE and the number of damaged areas (r^2=0.02, p=0.692) (data not shown).

Hippocampal atrophy in epileptic rats

In comparison to the control group, we found that hippocampal atrophy in the epileptic animals corresponds to 25% (p<0.001, Student's t-test) (Fig. 4E-F). There was not a significant correlation between hippocampal atrophy and the latency to develop SRSs (r^2=0.09, p=0.555) (data not shown).

Relationship between seizures after the administration of KA and SRSs

Both nonconvulsive (Fig. 5A-B, on the top) and convulsive SRSs (Fig. 5A-B, on the bottom) were considered in relation to SE progression. We did not find any relationship between: (i) the first stage 0-3 seizures developing after the KA injection and the latency to develop SRSs in chronic epilepsy (Fig. 5C-F); (ii) the latency to develop SE, or alternatively its duration (including the percentage of time spent in convulsive SE over the total SE duration), and the latency to develop SRSs in chronic epilepsy (Fig. 5G-N). In contrast, the latency to develop the first stage 5 CS after KA injection was positively related, respectively, to the latency to develop the first SRS in chronic epilepsy (r^2=0.60, p<0.001) (Fig. 5O), and the mean latency to develop the first stage 4-5 SRSs (r^2=0.44, p<0.001) (Fig. 5P). We also found a relationship between the latency to develop the first SRS and the mean latency to develop the first stage 4-5 SRSs (r^2=0.57, p<0.001) (Fig. 5Q). Finally, no relationship was found between the duration of SE and the seizure frequency 9 weeks after KA administration (r^2=0.14, p=0.176) (data not shown).

Discussion

In the present study, analysis of v-ECoG recordings and lesion extension resulted in the following major findings: i) the early increase of gamma power, which precedes the onset of SE, and the subsequent quick stabilization to under-the-baseline levels until the end of SE, both suggest a predominant role of this ECoG band in determining the overall SE duration; ii) the progressive increase in theta power during SE, reaching the peak in coincidence with the maximal duration of stage 4 CSs and immediately followed by a reduction when stage 5 CSs fully developed, both suggest a role of this band in determining the SE severity; iii) the overall duration of most severe seizures in the course of SE appears to correlate with the brain damage, without affecting the timing of epileptogenesis; iv) the onset of first spontaneous epileptic activity, including both nonconvulsive and convulsive SRSs, is predicted by latency to develop stage 5 CS in the course of SE.

Our main purpose was to re-evaluate the relationship between the lesion extent and the onset of epileptogenesis. To this aim, we first evaluated if the overall duration of CSE and the number of lesions were positively related, finding a significant result. Then, we assumed that a significant relationship should be also found for epileptogenesis, to indicate that a more widespread damage is responsible for an earlier seizure onset in chronic epilepsy. To test this assumption, we evaluated the relationship between overall duration of CSE and onset of SRSs, which was not significant. Although we approached this issue in an indirect manner, our findings are in agreement with evidence obtained in the pilocarpine model showing that rats with a different SE duration, expected to present a different lesion extent [4, 5], had a similar SRS onset [7, 36]. However, it would be reasonable to expect that a longer SE might result in earlier appearance of SRSs, but this was not the case in our model. On the other hand, the SE certainly increases the risk to develop epilepsy in adult patients, but the relationship of such risk with the SE duration is not established [37].

Distribution of lesions caused by KA in our animals was partially consistent with the available knowledge on the model [38, 39]. For instance, damage to CA3 is commonly observed in KA-treated rats, but it is usually referred to CA3 Py, whereas in the majority of our animals we also found damage in the CA3 LMol, a feature previously reported only in pilocarpine-treated rats [4]. Additionally, we observed that all rats with no exception presented a characteristic lesion in the Sub, in proximity to CA1. This region presents a two-way exchange of information with the Re of the thalamus [40, 41], which was also damaged in many examined animals. This suggests that the mentioned thalamic-subicular circuit is strongly affected by KA-induced SE so to produce a damage more extensive than that previously found [42]. Indeed, a widespread distribution of injuries in KA-treated rats represents a limitation of the model because of the focal nature of lesions found in TLE

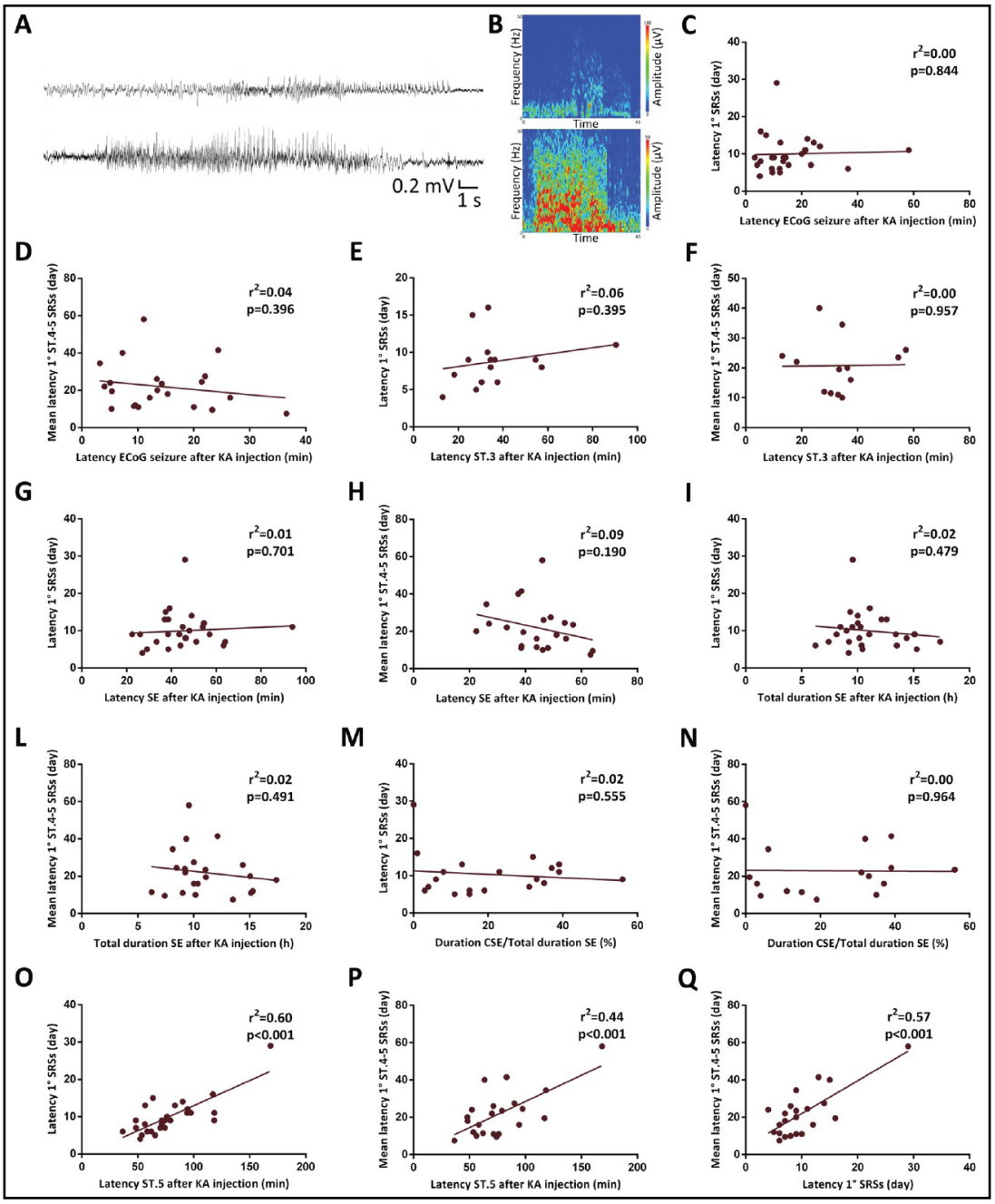

Fig. 5. Relationship between seizures after the administration of kainic acid (KA) and chronic epilepsy. In A, the first nonconvulsive (top) and the first convulsive spontaneous recurrent seizures (SRSs) (bottom) were reported. In B, the amplitude spectrum maps were shown for the first nonconvulsive (top) and the first convulsive SRSs (bottom). Relationships (r^2) between the first electrocorticographic seizure after KA injection and SRSs were determined in C-D, while relationships between the first stage (st.) 3 seizure after KA injection and SRSs were determined in E-F. Relationships between the latency to develop status epilepticus (SE) and SRSs were determined in G-H, whereas relationships between the total duration of SE and SRSs were determined in I-L. Similarly, relationships between the percentage of time spent in convulsive SE over the total SE duration and SRSs were determined in M-N. Moreover, relationships between the first st. 5 seizure after KA injection and SRSs were determined in O-P, while the relationship between the latency to develop the first SRS and the mean latency to develop the first convulsive (st. 4-5) SRS was determined in Q. Statistical analysis was performed using a linear regression analysis. Scale: 0.2 mV/1 s. CSE, convulsive status epilepticus; ECoG, electrocorticography.

patients, so to induce the development of other different experimental approaches to model TLE [39, 43]. However, the mentioned alternative approaches did not offer the possibility to address the relationship between SE and epileptogenesis, as instead required by our aims.

According to our aims, we also evaluated the impact of the SE dynamics on onset of SRSs. A growing number of studies suggest that early events occurring already during or immediately after SE could exert long-term morphological and functional effects, thus affecting the onset of seizure activity [44]. In our experiments, we found that the latency to the first CS with loss of posture in the course of SE was able to predict the onset of SRSs, so the timing of epileptogenesis. This result suggests that any pharmacological intervention able to delay the onset of tonic-clonic seizures during SE could have the potential to delay epileptogenesis. If correct, this means that drugs displaying such an effect may be potentially disclosed for their antiepileptogenic potential in the KA model of SE.

Our findings also indicate that theta and gamma components of cerebral electrical activity can play an important role in determining, respectively, the development of CSE and the overall duration of SE. In our animal model, theta activity might have played a role in promoting stage 4 seizures after SE induction, as its increase in power paralleled the changes in duration of stage 4 seizures and both peaked at the same time. However, when the theta power went back to baseline, CSE became more severe since stage 5 seizures peaked in duration, thus suggesting that a reduction in theta power precedes a full development of CSE. This is in agreement with experiments showing that induction of theta activity in the hippocampus counteracts the development of seizures [45–47]. Other authors also found a role for theta activity in determining the intensity of SE in knockout mice for the transient receptor potential canonical type 3 channel, in which pilocarpine-induced theta power and seizure scores were both reduced during the pre-ictal phase and SE phase [48]. Additionally, the theta band can play a role in the onset of SRSs after the SE, because it was found to be inversely correlated with the latency period and with the power change of the high-gamma rhythm in 3 mouse and 2 rat models of epileptogenesis [49].

Gamma activity originates from reciprocal connections of interneurons and principal cells, with a major role played by fast spiking parvalbumin interneurons [50, 51]. *In vitro* experiments provided evidence for a modulation of gamma oscillations by GABAergic and glutamatergic inputs. Interestingly, GABA type A ($GABA_A$) receptor activation increased the gamma power and, consistently, $GABA_A$ receptor antagonism resulted in the opposite finding. Gamma power increased also in presence of $GABA_B$ receptor antagonism. Additionally, blockade of the glutamate AMPA receptor reduced the gamma power, which was conversely increased by blocking metabotropic or NMDA glutamatergic receptors [52]. Although we did not perform any pharmacological experiment to assess the basis of changes observed in gamma power during the SE in our animals, it is conceivable that a dysfunction in GABAergic inhibitory activity could be responsible for the observed durable reduction in gamma power occurring in the entire course of SE, as suggested by experiments showing an anti-ictogenic role of parvalbumin interneurons during the SE [53]. Conversely, these same experiments revealed a paradoxical capacity to promote seizures of parvalbumin interneurons prior to the SE onset, which could also explain the increase in gamma power anticipating NCSE in our animals.

Conclusion

Overall, our study suggests that the analysis of SE dynamics is useful to identify various biomarkers that are predictive of SE progression, the resulting damage, and subsequent epileptogenesis. These biomarkers characterizing the SE dynamics could be useful to disclose new possible targets for more effective therapeutic approaches in TLE.

Acknowledgements

Dr. A.M. Costa is recipient of a fellowship from the Fondazione Mariani (Milan, Italy; grant R-19-110 to GB). Dr. C. Lucchi is recipient of a fellowship from the Department of Biomedical, Metabolic and Neural Sciences of the University of Modena and Reggio Emilia ("Progetto Dipartimento di Eccellenza 2018-2022").

Author Contributions

A.M.C., C.L., and G.B. designed experiments. A.M.C, C.L., and C.S. collaborated to data acquisition. A.M.C., and G.B. analyzed and interpreted data. A.M.C., and G.B. drafted the article. A.M.C., C.L., C.S, Í.R.L., and G.B. critically revised and finally approved the manuscript.

Statement of Ethics

Animal experiments conform to internationally accepted standards and have been approved by the appropriate institutional review body.

Funding

This study was supported by the Italian Ministry of Health (grant RF-2011-02350485 to GB), the University of Modena and Reggio Emilia (FAR2018 to GB), and BPER (project "Medicina Clinica e Sperimentale per il Trattamento delle Epilessie" to GB).

Disclosure Statement

The authors have no conflicts of interest to declare.

References

1 Mathern GW, Cifuentes F, Leite JP, Pretorius JK, Babb TL: Hippocampal EEG excitability and chronic spontaneous seizures are associated with aberrant synaptic reorganization in the rat intrahippocampal kainate model. Electroencephalogr Clin Neurophysiol 1993;87:326–339.

2 Pitkänen A, Lukasiuk K, Dudek FE, Staley KJ: Epileptogenesis. Cold Spring Harb Perspect Med 2015;5:pii:a022822.

3 Morimoto K, Fahnestock M, Racine RJ: Kindling and status epilepticus models of epilepsy: rewiring the brain. Prog Neurobiol 2004;73:1–60.

4 Biagini G, Baldelli E, Longo D, Contri MB, Guerrini U, Sironi L, et al.: Proepileptic influence of a focal vascular lesion affecting entorhinal cortex-CA3 connections after status epilepticus: J Neuropathol Exp Neurol 2008;67:687–701.

5 Klitgaard H, Matagne A, Vanneste-Goemaere J, Margineanu DG: Pilocarpine-induced epileptogenesis in the rat: impact of initial duration of status epilepticus on electrophysiological and neuropathological alterations. Epilepsy Res 2002;51:93–107.

6 Lemos T, Cavalheiro EA: Suppression of pilocarpine-induced status epilepticus and the late development of epilepsy in rats. Exp Brain Res 1995;102:423-428.

7 Bortel A, Lévesque M, Biagini G, Gotman J, Avoli M: Convulsive status epilepticus duration as determinant for epileptogenesis and interictal discharge generation in the rat limbic system. Neurobiol Dis 2010;40:478–489.

8 Drexel M, Preidt AP, Sperk G: Sequel of spontaneous seizures after kainic acid-induced status epilepticus and associated neuropathological changes in the subiculum and entorhinal cortex. Neuropharmacology 2012;63:806–817.

9 Lévesque M, Avoli M, Bernard C: Animal models of temporal lobe epilepsy following systemic chemoconvulsant administration. J Neurosci Methods 2016;260:45–52.

10 Henshall DC: Poststatus epilepticus models: focal kainic acid, in: Pitkänen A, Buckmaster PS, Galanopoulou A, Solomon LM (eds): Models of seizures and epilepsy. London, Elsevier Academic, 2017, ed 2, pp 611–624.

11 Dudek FE, Clark S, Williams PA, Grabenstatter HL: Kainate-induced status epilepticus: a chronic model of acquired epilepsy, in: Pitkänen A, Schwartzkroin PA, Moshe SL (eds): Models of seizures and epilepsy. Boston, Elsevier Academic, 2006, pp 415–432.
12 Dudek FE, Staley KJ: Post-status epilepticus models: systemic kainic acid, in: Pitkänen A, Buckmaster PS, Galanopoulou A, Solomon LM (eds): Models of seizures and epilepsy. London, Elsevier Academic, 2017, ed 2, pp. 599–610.
13 Trinka E, Cock H, Hesdorffer D, Rossetti AO, Scheffer IE, Shinnar S, et al.: A definition and classification of status epilepticus - Report of the ILAE Task Force on classification of status epilepticus. Epilepsia 2015;56:1515–1523.
14 Lucchi C, Costa AM, Giordano C, Curia G, Piat M, Leo G, et al.: Involvement of PPARγ in the anticonvulsant activity of EP-80317, a ghrelin receptor antagonist. Front Pharmacol 2017;8:676.
15 Kadam SD, D'Ambrosio R, Duveau V, Roucard C, Garcia-Cairasco N, Ikeda A, et al.: Methodological standards and interpretation of video-electroencephalography in adult control rodents. A TASK1-WG1 report of the AES/ILAE Translational Task Force of the ILAE. Epilepsia 2017;58:10–27.
16 Pitsch J, Becker AJ, Schoch S, Müller JA, de Curtis M, Gnatkovsky V: Circadian clustering of spontaneous epileptic seizures emerges after pilocarpine-induced status epilepticus. Epilepsia 2017;58:1159–1171.
17 D'Ambrosio R, Miller JW: What is an epileptic seizure? unifying definitions in clinical practice and animal research to develop novel treatments. Epilepsy Curr 2010;10:61–66.
18 Racine RJ: Modification of seizure activity by electrical stimulation: II. Motor seizure. Electroencephalogr Clin Neurophysiol 1972;32:281–294.
19 Lowenstein DH: Status epilepticus: an overview of the clinical problem. Epilepsia 1999;40 S1:S3-S8.
20 Williams PA, White AM, Clark S, Ferraro DJ, Swiercz W, Staley KJ, et al.: Development of spontaneous recurrent seizures after kainate-induced status epilepticus. J Neurosci 2009;29:2103–2112.
21 Kemp B, van Beelen T, Stijl M, van Someren P, Roessen M, van Dijk JG: A DC attenuator allows common EEG equipment to record fullband EEG, and fits fullband EEG into standard European Data Format. Clin Neurophysiol 2010;121:1992–1997.
22 Bouyer JJ, Montaron MF, Rougeul A: Fast fronto-parietal rhythms during combined focused attentive behaviour and immobility in cat: cortical and thalamic localizations. Electroencephalogr Clin Neurophysiol 1981;51:244–252.
23 Klimesch W, Doppelmayr M, Schimke H, Ripper B: Theta synchronization and alpha desynchronization in a memory task. Psychophysiology 1997;34:169–176.
24 Kahana MJ, Sekuler R, Caplan JB, Kirschen M, Madsen JR: Human theta oscillations exhibit task dependence during virtual maze navigation. Nature 1999;399:781–784.
25 Jensen O, Tesche CD: Frontal theta activity in humans increases with memory load in a working memory task: frontal theta increases with memory load. Eur J Neurosci 2002;15:1395–1399.
26 Canolty RT, Edwards E, Dalal SS, Soltani M, Nagarajan SS, Kirsch HE, et al.: High gamma power is phase-locked to theta oscillations in human neocortex. Science 2006;313:1626–1628.
27 Guderian S, Schott BH, Richardson-Klavehn A, Duzel E: Medial temporal theta state before an event predicts episodic encoding success in humans. Proc Natl Acad Sci U S A 2009;106:5365–5370.
28 Paré D: Amygdala oscillations and the consolidation of emotional memories. Trends Cogn Sci 2002;6:306–314.
29 Magill PJ, Sharott A, Bolam JP, Brown P: Delayed synchronization of activity in cortex and subthalamic nucleus following cortical stimulation in the rat: synchronized activity in cortex and subthalamic nucleus. J Physiol 2006;574:929–946.
30 Nerad L, McNaughton N: The septal EEG suggests a distributed organization of the pacemaker of hippocampal theta in the rat. Eur J Neurosci 2006;24:155–166.
31 DeCoteau WE, Thorn C, Gibson DJ, Courtemanche R, Mitra P, Kubota Y, et al.: Learning-related coordination of striatal and hippocampal theta rhythms during acquisition of a procedural maze task. Proc Natl Acad Sci U S A 2007;104:5644–5649.
32 Vinet J, Costa AM, Salinas-Navarro M, Leo G, Moons L, Arckens L, et al.: A hydroxypyrone-based inhibitor of metalloproteinase-12 displays neuroprotective properties in both status epilepticus and optic nerve crush animal models. Int J Mol Sci 2018;19:pii:E2178.

33 Giordano C, Costa AM, Lucchi C, Leo G, Brunel L, Fehrentz JA, et al.: Progressive seizure aggravation in the repeated 6-Hz corneal stimulation model is accompanied by marked increase in hippocampal p-ERK1/2 immunoreactivity in neurons. Front Cell Neurosci 2016;10:281.
34 Lucchi C, Vinet J, Meletti S, Biagini G: Ischemic-hypoxic mechanisms leading to hippocampal dysfunction as a consequence of status epilepticus. Epilepsy Behav 2015;49:47–54.
35 Gualtieri F, Curia G, Marinelli C, Biagini G: Increased perivascular laminin predicts damage to astrocytes in CA3 and piriform cortex following chemoconvulsive treatments. Neuroscience 2012;218:278–294.
36 Zhang X, Cui SS, Wallace AE, Hannesson DK, Schmued LC, Saucier DM, et al.: Relations between brain pathology and temporal lobe epilepsy. J Neurosci 2002;22:6052–6061.
37 Meierkord H: The risk of epilepsy after status epilepticus in children and adults. Epilepsia 2007;48:94–95.
38 Lévesque M, Avoli M: The kainic acid model of temporal lobe epilepsy. Neurosci Biobehav Rev 2013;37:2887–2899.
39 Schwob JE, Fuller T, Price JL, Olney JW: Widespread patterns of neuronal damage following systemic or intracerebral injections of kainic acid: a histological study. Neuroscience 1980;5:991–1014.
40 Wouterlood FG, Saldana E, Witter MP: Projection from the nucleus reuniens thalami to the hippocampal region: light and electron microscopic tracing study in the rat with the anterograde tracer Phaseolus vulgaris-leucoagglutinin. J Comp Neurol 1990;296:179–203.
41 McKenna JT, Vertes RP: Afferent projections to nucleus reuniens of the thalamus. J Comp Neurol 2004;480:115–142.
42 Drexel M, Preidt AP, Kirchmair E, Sperk G: Parvalbumin interneurons and calretinin fibers arising from the thalamic nucleus reuniens degenerate in the subiculum after kainic acid-induced seizures. Neuroscience 2011;189:316–329.
43 Sloviter RS, Bumanglag AV: Defining "epileptogenesis" and identifying "antiepileptogenic targets" in animal models of acquired temporal lobe epilepsy is not as simple as it might seem. Neuropharmacology 2013;69:3–15.
44 Klein P, Dingledine R, Aronica E, Bernard C, Blümcke I, Boison D, et al.: Commonalities in epileptogenic processes from different acute brain insults: Do they translate? Epilepsia 2018;59:37–66.
45 Izadi A, Pevzner A, Lee DJ, Ekstrom AD, Shahlaie K, Gurkoff GG: Medial septal stimulation increases seizure threshold and improves cognition in epileptic rats. Brain Stimulat 2019;12:735–742.
46 Colom LV, García-Hernández A, Castañeda MT, Perez-Cordova MG, Garrido-Sanabria ER: Septo-hippocampal networks in chronically epileptic rats: potential antiepileptic effects of theta rhythm generation. J Neurophysiol 2006;95:3645–3653.
47 Miller JW, Turner GM, Gray BC: Anticonvulsant effects of the experimental induction of hippocampal theta activity. Epilepsy Res 1994;18:195–204.
48 Phelan KD, Shwe UT, Cozart MA, Wu H, Mock MM, Abramowitz J, et al.: TRPC3 channels play a critical role in the theta component of pilocarpine-induced status epilepticus in mice. Epilepsia 2017;58:247–254.
49 Milikovsky DZ, Weissberg I, Kamintsky L, Lippmann K, Schefenbauer O, Frigerio F, et al.: Electrocorticographic dynamics as a novel biomarker in five models of epileptogenesis. J Neurosci 2017;37:4450–4461.
50 Buzsáki G, Wang XJ: Mechanisms of gamma oscillations. Annu Rev Neurosci 2012;35:203–225.
51 Wulff P, Ponomarenko AA, Bartos M, Korotkova TM, Fuchs EC, Bähner F, et al.: Hippocampal theta rhythm and its coupling with gamma oscillations require fast inhibition onto parvalbumin-positive interneurons. Proc Natl Acad Sci U S A 2009;106:3561–3566.
52 Johnson NW, Özkan M, Burgess AP, Prokic EJ, Wafford KA, O'Neill MJ, et al.: Phase-amplitude coupled persistent theta and gamma oscillations in rat primary motor cortex *in vitro*. Neuropharmacology 2017;119:141–156.
53 Lévesque M, Chen LY, Etter G, Shiri Z, Wang S, Williams S, et al.: Paradoxical effects of optogenetic stimulation in mesial temporal lobe epilepsy. Ann Neurol 2019;86:714–728.